



METABOLIC, ENDOCRINE, AND GENITOURINARY PATHOBIOLOGY

Gastric Bypass Surgery Reverses Diabetic Phenotypes in *Bdnf*-Deficient Mice



Shujun Jiang,^{*} Qinghua Wang,^{*†} Zan Huang,[‡] Anying Song,^{*} Yu Peng,[‡] Siyuan Hou,^{*} Shiyong Guo,^{*} Weiyun Zhu,[‡] Sheng Yan,[§] Zhaoyu Lin,^{*¶} and Xiang Gao^{*¶}

From the State Key Laboratory of Pharmaceutical Biotechnology and MOE Key Laboratory of Model Animal for Disease Study,^{*} Model Animal Research Center, Nanjing Biomedical Research Institute, and the Collaborative Innovation Center of Genetics and Development,[¶] Nanjing University, Nanjing; the Laboratory Animal Center,[†] Nantong University, Nantong; the Laboratory of Gastrointestinal Microbiology,[‡] Nanjing Agricultural University, Nanjing; and the First Hospital of Zhejiang Province,[§] First Affiliate Hospital, Zhejiang University, Hangzhou, China

Accepted for publication
April 11, 2016.

Address correspondence to
Xiang Gao, Ph.D., or Zhaoyu
Lin, Ph.D., State Key Laboratory of Pharmaceutical
Biotechnology and MOE Key
Laboratory of Model Animal
for Disease Study, Model Ani-
mal Research Center, Nanjing
Biomedical Research Institute,
Nanjing University, 12 Xuefu
Rd., Pukou District, 210061
Nanjing, China. E-mail:
gaoxiang@nju.edu.cn or
linzy@nju.edu.cn.

Duodenum-jejunum gastric bypass (DJB) has been used to treat morbid diabetic patients. However, neither the suitability among patients nor the mechanisms of this surgical treatment is clear. Previously, we reported a new mouse strain named *Timo* as type 2 diabetes model caused by brain-derived neurotrophic factor (*Bdnf*) deficiency. In this study, we found that DJB on *Timo* mice reversed their metabolic abnormalities without altering the expression of *Bdnf*. Glucose tolerance and insulin sensitivity were improved greatly, along with reduction of fat accumulation in liver and white adipose tissue. The gut flora population was altered by DJB with increased proportion of Firmicutes and decreased Actinobacteria and Proteobacteria in the ileum after surgery. Systemic inflammation in *Timo* mice was greatly suppressed with less macrophage infiltration and lower tumor necrosis factor- α levels in liver and white adipose tissue after surgery. Interestingly, the alteration of gut microflora abundance and improved metabolism preceded the inflammation alleviation after DJB surgery. These results suggested that DJB can reverse *Bdnf* deficiency-associated metabolic abnormality. In addition, the reduced inflammation may not be the initial cause for the DJB-associated metabolic and microbiota alterations. The increased BDNF protein levels in hypothalamus and hippocampus may result from microbiota change after DJB surgery. (*Am J Pathol* 2016, 186: 2117–2128; <http://dx.doi.org/10.1016/j.ajpath.2016.04.009>)

Surgical treatment, especially bariatric surgery, was proposed as an effective method to maintain long-term weight loss and remission of type 2 diabetes mellitus (T2DM), in addition to lifestyle and pharmacologic interventions.^{1–3} Diabetes remission appears before weight reduction in patients who undergo Roux-en-Y gastric bypass surgery. Therefore, it is unlikely that weight loss is the factor that improves insulin sensitivity.⁴ Other hypotheses of this effect of duodenum-jejunum gastric bypass (DJB) require more direct evidence. For example, Dirksen et al⁵ suggested that an accelerated transit of concentrated nutrients (particularly glucose) to the distal intestine results in the increased production of insulinotropic and appetite-controlling substances. However, there are conflicting reports on the changes in gut hormone levels after bariatric surgery.^{6–8} Low-grade inflammation in adipose tissue and liver is one of the primary causes for low insulin sensitivity in obesity and

T2DM.^{9–12} Several recent studies found that decreased adiposity and increased insulin sensitivity after surgery was associated with gut microbiota alterations.^{3,13,14} However, how rapid changes in gut microbiota result in glycemic improvements and alterations in metabolites are not clear.

Suppression of systemic inflammation in mice and humans is associated with an increased abundance of potentially proinflammatory Proteobacteria, Bacteroides, and *Ruminococcus gnavus* in gut.¹⁵ Decreased Lachnospiraceae and

Supported by Ministry of Science and Technology of China grants 2011BAI15B02, 2014BAI02B01, and 2015BAI08B02 (X.G.); National Natural Science Foundation of China grant 31301217 (Z.L.); and Natural Science Foundation of the Jiangsu Higher Education Institutions of China grant no. 11KJB180010 (Q.W.).

S.J. and Q.W. contributed equally to this work.

Disclosures: None declared.

Bifidobacterium abundance also correlates with reduced butyrate content in obese humans.^{15,16} Populations of Enterobacteriales and Verrucomicrobiales were increased in mice after Roux-en-Y gastric bypass surgery compared with sham mice.¹⁴ Increased Proteobacteria and decreased Firmicutes and Bacteroidetes were observed in Roux-en-Y gastric bypass rats.¹⁷ Previous studies of gut microflora before and after gastric bypass revealed reciprocal changes in Bacteroidetes and Firmicutes, but alterations in the Bacteroidetes/Firmicutes ratio varied in different reports.^{3,18} Some studies demonstrated that bacteria directly promoted gut inflammation and insulin resistance in mice fed a high-fat diet (HFD).^{19,20}

Timo mutant strain was generated in our laboratory as a T2DM animal model induced by *Bdnf* deficiency, in which a conserved genomic locus of *Bdnf* is disrupted by a *trans* gene insertion that decreases brain-derived neurotrophic factor (BDNF) levels to 30% of wild-type mice. *Timo* mice exhibit insulin resistance, hyperlipidemia, and metabolic inflammation before the onset of obesity and diabetes.²¹ However, whether the DJB surgery can reverse the metabolic phenotypes of *Timo* mutants is not known. In addition, *Timo* mice may also serve as a good model to investigate how inflammation and microbiota regulate insulin sensitivity and glucose metabolism after DJB surgery. In this study, we demonstrated that DJB surgery improved glyce-mic homeostasis and insulin sensitivity in *Timo* mice. We also observed alterations in gut microbiota before reduced inflammation and increased BDNF in *Timo* mice.

Materials and Methods

Animals and Duodenum-Jejunum Gastric Bypass Surgery

Timo mice were generated in our laboratory as described previously,²¹ and male C57BL/6J mice were housed in a specific pathogen-free facility under 12-hour light-dark cycle and hydrated with acidified water at the Model Animal Research Center of Nanjing University. *Timo* mice were fed a standard chow diet *ad libitum*. Seven-week-old male wild-type C57BL/6J mice were fed a HFD for 17 weeks before surgery or a normal chow diet as control. The Institutional Animal Care and Use Committee of the Model Animal Research Center of Nanjing University approved the experimental protocols.

Ten-week-old *Timo* mice and HFD-induced C57BL/6J mice underwent DJB surgery as previously described.²² Mice were deprived of food overnight before surgery and anesthetized with intraperitoneal 1.25% Avertin (T48402; Sigma-Aldrich, St. Louis, MO). All mice received 100 μ L 0.5% carprofen subcutaneously to alleviate discomfort after surgery.

Insulin and Glucose Tolerance Test

Timo mice were deprived of food 16 hours before the oral glucose [D (+)-glucose; Sigma-Aldrich] tolerance test

(2 g/kg body weight). Blood glucose concentrations were tested at 0, 15, 30, 60, 90, and 120 minutes after glucose administration. Mice were injected with 0.5 U of insulin for 1 kg body weight after a 6-hour food deprivation for the insulin tolerance test (Novo Nordisk Pharmaceutical Industries, Malov, Denmark), and blood glucose concentrations were measured at 0, 15, 30, 60, 90, and 120 minutes after insulin injection. Blood concentrations were tested using a Breeze 2 Blood Glucose Meter (Bayer HealthCare LLC, Mishawaka, IN). Body weight was measured weekly at the same time point.

Metabolic Measurements

Blood was collected from *Timo* mice eye socket veins after overnight food deprivation in heparinized tubes, and samples were stored at room temperature for 30 minutes to separate serum from whole blood. Serum was collected after centrifugation at $3000 \times g$ for 15 minutes. Plasma (10 μ L) was used to measure insulin concentrations using a mouse insulin enzyme-linked immunosorbent assay kit (Millipore, Billerica, MA; catalog no. EZRMI-13K), according to the manufacturer's instruction. Plasma concentrations of leptin were determined using a mouse leptin enzyme-linked immunosorbent assay kit (Millipore; catalog no. EZRMI-82K). Plasma BDNF levels were detected using a BDNF enzyme-linked immunosorbent assay kit (Boatman Tech, Shanghai, China).

Blood Chemistry for Lipid Metabolism

Lipid metabolites and hepatitis concentrations, including total cholesterol, triglycerides, high-density lipoprotein, very-low-density lipoprotein, alanine aminotransferase, and aspartate aminotransferase, in plasma of *Timo* mice after DJB surgery were quantified using colorimetric assays in a 7020 automatic analyzer (Hatachi High Technology, Tokyo, Japan). Food intake and energy expenditure were measured using a complementary laboratory animal metabolic system.

Histologic Analyses

Liver and adipose tissues were fixed in 4% paraformaldehyde and embedded in paraffin. Sections (5 mm) were generated using a Leica (Wetzlar, Germany) microtome (RM2155) and stained with hematoxylin and eosin according to standard procedures. Liver frozen sections (10 mm) were stained with Oil Red O to analyze lipid accumulation.

Quantitative RT-PCR Analyses

High-quality total RNA from liver, white adipose tissue (WAT), brown adipocyte tissue (BAT), and muscle was isolated by extraction with RNAiso plus (9108; TaKaRa, Tokyo, Japan). cDNA was synthesized using a PrimeScript RT reagent Kit with a gDNA Eraser kit (RR047A; TaKaRa). The primers used for *F4/80*, *Cd11b*, *Cd11c*,

tumor necrosis factor- α (*Tnfa*), IL-6 (*Il6*), IL-1 β (*Il1b*), and monocyte chemoattractant protein 1 (*Mcp1*), and 36B4 were as follows: F4/80, 5'-AGTACGATGTGGG-GCTTTTG-3' (forward) and 5'-CCCCATCTGTACATC-CCACT-3' (reverse); Cd11b, 5'-CAGTTCCCAGAGGC-TCTCA-3' (forward) and 5'-GGAGCCATCAATCAA-GAAG-3' (reverse); Cd11c, 5'-ATGGAGCCTCAAGA-CAGGAC-3' (forward) and 5'-GGATCTGGGATGCT-GAAATC-3' (reverse); Mcp-1, 5'-CATCCACGTGTTG-GCTCA-3' (forward) and 5'-GATCATCTTGCTGGT-GAATGAGT-3' (reverse); Tnf- α , 5'-CTTCTCATTC-CTGCTTGTGG-3' (forward) and 5'-GGTCTGGGGCA-TAGAACTGA-3' (reverse); Il-1 β , 5'-AACCTGCTGGT-GTGTGACGTTCC-3' (forward) and 5'-AGCACGAGGCT-TTTTTGTTGT-3' (reverse); and Il-6, 5'-CGCTATGAA-GTTCCTCTCTGC-3' (forward) and 5'-CCTCTGTGA-AGTCTCCTCTCC-3' (reverse). Quantitative reverse transcription-PCR for each gene was performed using SYBR Premix Ex Taq (RR420A; TaKaRa) in an ABI 7700 sequence detector (Applied Biosystems, Foster City, CA). The relative abundance of target gene transcripts was normalized to 36B4 expression.

Western Blot Analysis

Total protein extracts from WAT, liver, hypothalamus, and hippocampus were homogenized in RIPA lysis buffer that contained a 1% protease inhibitor cocktail (Sigma-Aldrich) and a 1% tyrosine phosphatase inhibitor cocktail (Sigma-Aldrich). Immunoblotting was performed as previously described.²³ Total TNF- α was immunoblotted using a rat anti-TNF- α antibody (BD Biosciences, San Jose, CA; catalog no. 559064). Total BDNF was immunoblotted using a rabbit anti-BDNF antibody (Santa Cruz Biotechnology, Santa Cruz, CA; sc-546).

TNF- α Injection and Measurement

Plasma TNF- α levels were determined using a mouse TNF- α enzyme-linked immunosorbent assay kit (MTA00B; R&D Systems, Minneapolis, MN), according to the manufacturer's protocol. Mouse recombinant TNF- α (10 μ g/kg) (GenScript, Nanjing, China; Z02918-100) was continuously injected intraperitoneally into *Timo* mice for 7 days after DJB surgery.

Bacterial DNA Extraction

Fecal samples and different parts of the biliopancreatic limb, the Roux limb, ileum, cecum, colon, and rectum were collected from DJB and sham mice and stored at -80°C for further use. Bacterial genomic DNA was extracted using the QiaAmp DNA stool Mini DNA-Isolation Kit (Qiagen, Hilden, Germany) according to the manufacturer's protocol. Concentrations were measured using the Qubit 2.0 instrument and the Qubit dsDNA HS Assay (Life Technologies, Invitrogen Division, Darmstadt, Germany).

16S rRNA Gene Primer and Amplicon Library Construction

Primers were used to amplify the 16S rRNA hyper variable region V6 according to the report by Huber et al²⁴; all primers sequences are as follows: 967F-PP, 5'-CNACGC-GAAGAACCTTANC-3'; 967F-UC1, 5'-CAACGCGAA-AAACCTTACC-3'; 967F-UC2, 5'-CAACGCGCAGAAC-CTTACC-3'; 967F-UC3, 5'-ATACGCGARGAACCTTACC-3'; 967F-AQ, 5'-CTAACCGANGAACCTYACC-3'; 1046R, 5'-CGACAGCCATGCANCACCT-3'; 1046R-PP, 5'-CGACAACCATGCANCACC-3'; 1046R-AQ1, 5'-CGACGCGCCATGCANCACCT-3'; and 1046R-AQ2, 5'-CGACGACCATGCANCACCT-3'. The generated amplicon libraries were used in the Ion Plus Fragment Library Kit (Life Technologies, Invitrogen Division; catalog no. 4471252) according to the manufacturer's instructions. Library concentrations were measured using the Qubit 2.0 instrument and the Qubit dsDNA HS Assay (Life Technologies, Invitrogen Division).

Microbiota 16S rRNA Gene Sequencing and Analysis

The Ion Torrent Personal Genome Machine Template OT2 200 kit (Life Technologies; catalog no. 4480974) was applied to perform emulsion PCR using the Ion OneTouch 2 system as described in the User Guidelines (Part No. 4469004 Rev. B 07/2011). Amplicon libraries were sequenced on the Ion Torrent Personal Genome Machine system using the Ion Torrent Personal Genome Machine Sequencing 200 Kit v2 (catalog no. 4482006; Life Technologies) according to the manufacturer's protocol. The sphere was loaded to a 316 chip (Life Technologies) according to the method of Sebastian.²⁵ Shanghai Biotechnology Corporation (Shanghai, China) analyzed 16S rRNA gene sequences. The relative abundance of bacterial taxonomic groups was compared in all sequences, and a principal coordinate's analysis plot of weighted UniFrac distances was also performed in different groups.

Denaturing Gradient Gel Electrophoresis

Fecal bacteria DNA (100 ng) was amplified by 16rRNA v6-v8 variation region primers (968F primer contains GC clamp: 5'-CGCCCGGGGCGCGCCCCGGGCGGGGCGGGGGCAG-GGGAACGCGAAGAACCTTAC-3'; 1401R primer: CG-GTGTGTACAAGACCC) using a 2X Taqplus Master Polymerase mix (Vazyme; P212-01/02/03), 433-bp amplicon was generated. Eight percent acrylamide gel (acrylamide:bisacrylamide, 37.5:1) with a 35% to 55% (w/v) urea denaturant gradient was run at 80V for 12 hours. The gels were stained by 2 mg/mL silver in Cairns' fixation solution, and 1.5% NaOH that contained 0.4% formaldehyde as developer. The special band was extracted, transformed into *Escherichia*

coli with PMD19-T vector (TaKaRa; catalog no. 6013), sequenced, and compared using BLAST (National Center for Biotechnology Information, <http://www.ncbi.nlm.nih.gov>, last accessed March 19, 2016).

Statistical Analysis

Statistically significant differences between *Timo* mice and wild-type littermates are presented as means \pm SEM. All data were analyzed using one-way analysis of variance (when three groups are compared) or repeated measurement analysis of variance (for time course data) and unpaired Student's *t*-test. $P < 0.05$ was considered significant.

Results

Obesity, Glucose Intolerance, and Insulin Insensitivity in *Timo* Mice Are Reversed after DJB Surgery

Timo mice exhibited obesity, diabetes, and inflammation at 4 weeks of age (Supplemental Figure S1). To investigate whether DJB surgery reversed obesity in *Timo* mice, we performed DJB surgery on 10-week-old male *Timo* mice according to Woods et al²² (Supplemental Figure S2). We found that DJB surgery caused a decrease in body weight from 34.99 ± 4 g to 26.59 ± 3.14 g after 1 week in *Timo* mice (Figure 1, A–C). HFD-induced obese mice, as a positive control, also exhibited body weight loss from 40.88 ± 0.18 g to 31.55 ± 0.79 g 1 week after surgery, and

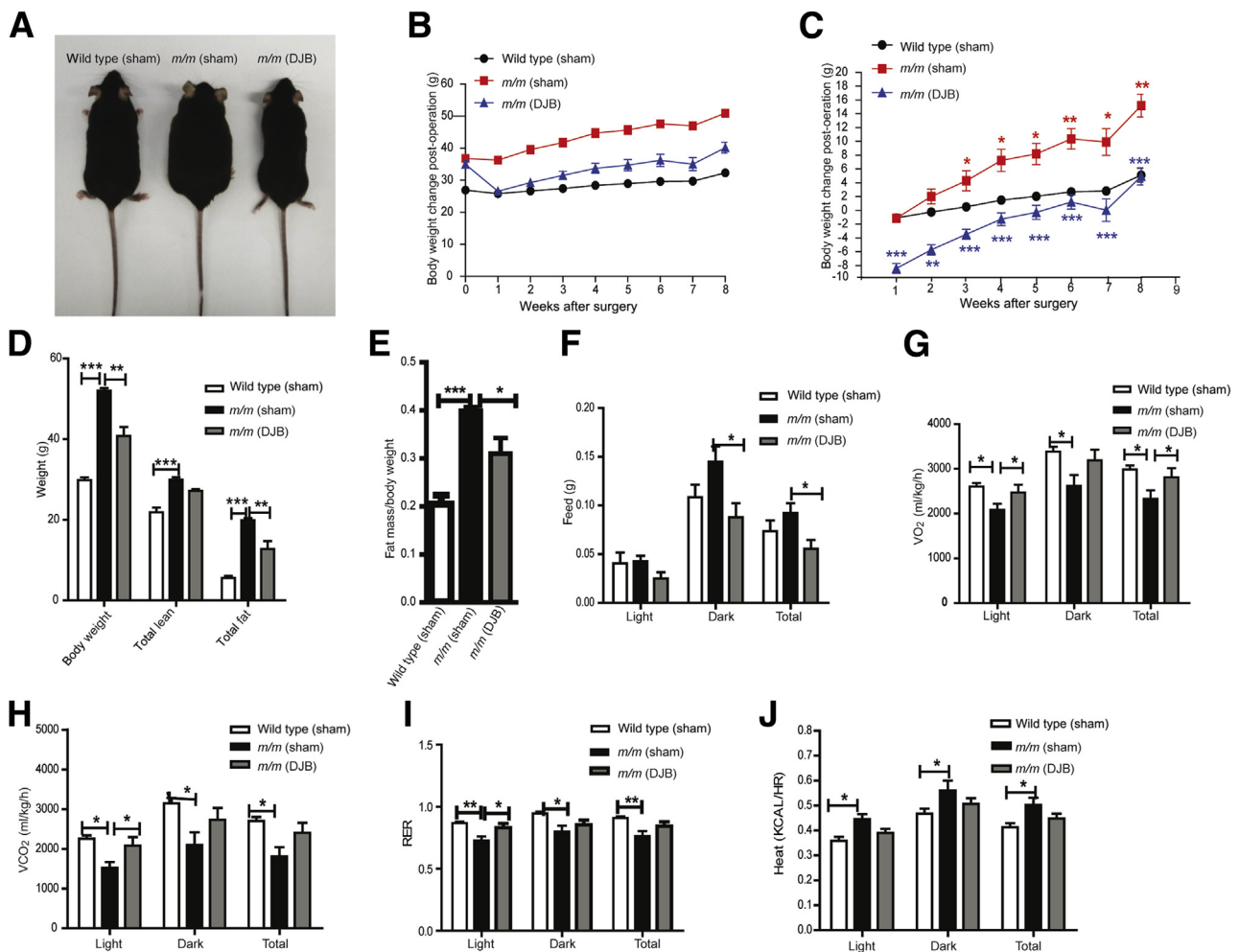


Figure 1 Body weight and metabolism phenotypes of male *Timo* mice decrease after DJB surgery. **A:** Body weight of 10-week-old male severely obese *Timo* mice decreases 8 weeks after surgery. **B:** Weekly body weights for each of the sham and DJB mice. **C:** Relative body weight changes in the sham group and DJB group after DJB surgery. **D** and **E:** Fat and lean mass of *Timo* mice 8 weeks after DJB surgery by dual-energy X-ray absorptiometry analysis. **F:** Food intake of *Timo* mice 6 weeks after DJB surgery by complementary laboratory animal metabolic system. **G:** VO_2 of *Timo* mice 6 weeks after DJB surgery by complementary laboratory animal metabolic system. **H:** VCO_2 per kilogram of lean body weight of *Timo* mice 6 weeks after DJB surgery by complementary laboratory animal metabolic system. **I:** RER of *Timo* mice 6 weeks after DJB surgery by complementary laboratory animal metabolic system. **J:** Heat production of *Timo* mice 6 weeks after DJB surgery by complementary laboratory animal metabolic system. Data are expressed as means \pm SEM. $n = 8$ to 13 (**A**); $n = 5$ (**J**). * $P < 0.05$, ** $P < 0.005$, and *** $P < 0.001$. DJB, duodenum-jejunum gastric bypass; RER, respiratory exchange ratio (VCO_2/VO_2); VCO_2 , carbon dioxide release; VO_2 , oxygen consumption.

exhibited better control of glucose (Supplemental Figure S3). Decreased body weight in *Timo* mice directly correlated with reductions in fat mass (Figure 1, D and E). *Timo* mice consumed fewer calories but exhibited no differences in physical activity from that of sham mice 8 weeks after DJB surgery (Figure 1, F–J, and Supplemental Figure S4). Our data confirm that DJB significantly reduced body weights in *Timo* mice and reduced food intake.

Bariatric surgery is one of the new clinical treatments for severe T2DM.^{26,27} Insulin sensitivity was normalized to the level of wild-type littermates 2 weeks after DJB surgery (Figure 2A). The effect of DJB surgery on insulin sensitivity was maintained for at least 8 weeks (Figure 2, B and C). Plasma insulin concentrations were reduced to normal concentrations in DJB *Timo* mice compared with sham wild-type littermates 9 weeks after DJB surgery (Figure 2D). The

correction of glucose intolerance in *Timo* mice was maintained for at least 8 weeks after surgery (Figure 2, E and F).

Lipid Accumulation Is Reduced in *Timo* Mice after DJB Surgery

Obesity and T2DM are accompanied by leptin resistance because lipid accumulation damages leptin signaling.^{28,29} Lipid accumulation in liver and adipose tissue (WAT and BAT) and enlarged adipocyte size occurred in 8-week-old male *Timo* mice (Figure 3A). *Timo* mice also exhibited a tendency for leptin resistance with increased concentrations at 6 weeks (Supplemental Figure S5A).

Histologic analyses and Oil Red O staining revealed that fat content decreased significantly in the livers of *Timo* mice 8 weeks after surgery compared with that of the sham *Timo* mice (Figure 3B). Hepatitis (alanine aminotransferase) was

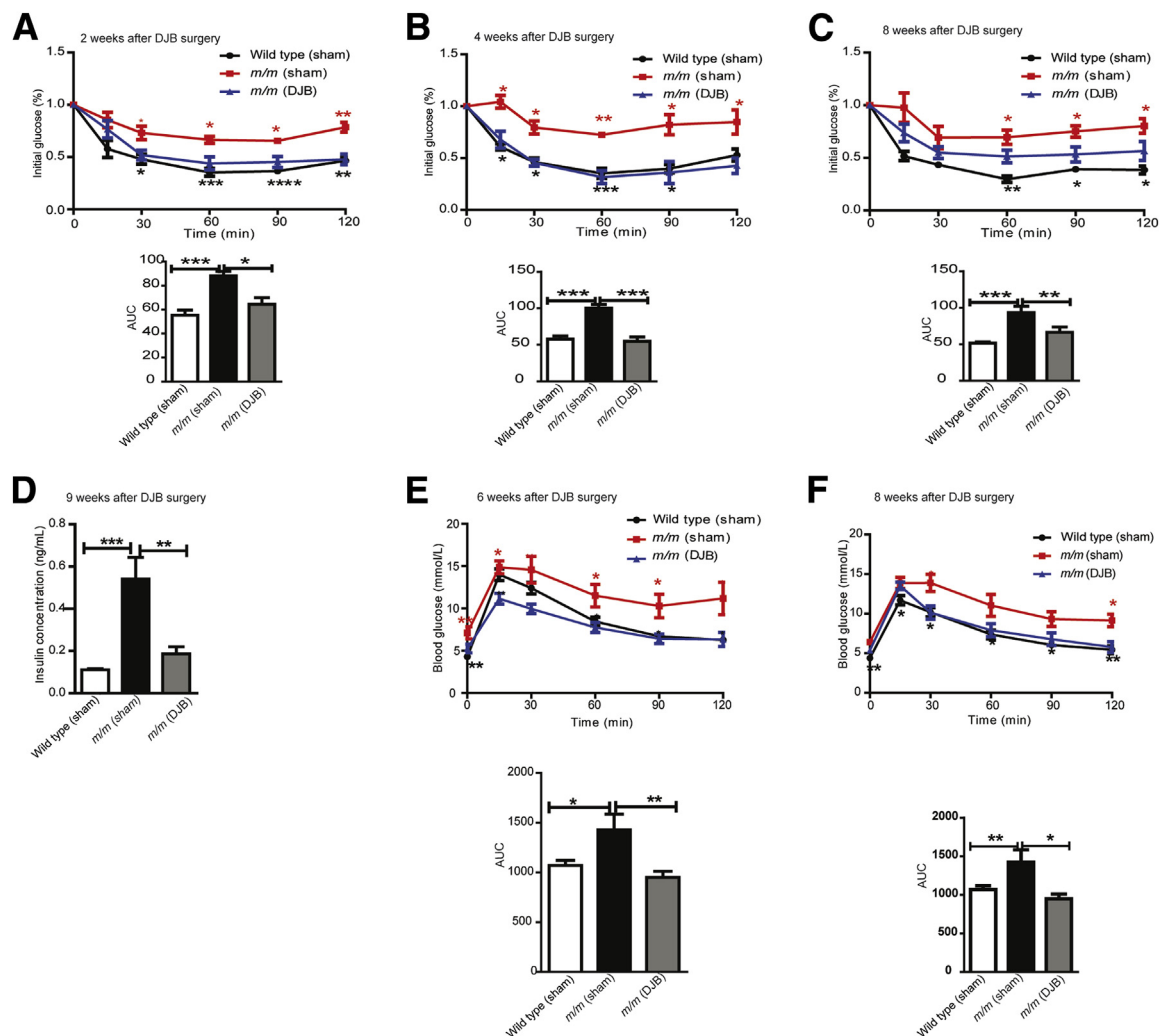


Figure 2 Insulin sensitivity increases after DJB surgery in male *Timo* mice. **A–C:** Insulin tolerance improves 2 (**A**), 4 (**B**), and 8 (**C**) weeks after DJB surgery by insulin tolerance test. **D:** Plasma insulin concentration decreases to normal after DJB surgery for 9 weeks by enzyme-linked immunosorbent assay. **E and F:** Oral glucose tolerance increases 6 and 8 weeks after DJB surgery by glucose tolerance test. Data are expressed as means \pm SEM. $n = 3$ to 7 (**E** and **F**). * $P < 0.05$, ** $P < 0.005$, *** $P < 0.001$, and **** $P < 0.0005$. AUC, area under the curve; DJB, duodenum-jejunum gastric bypass.

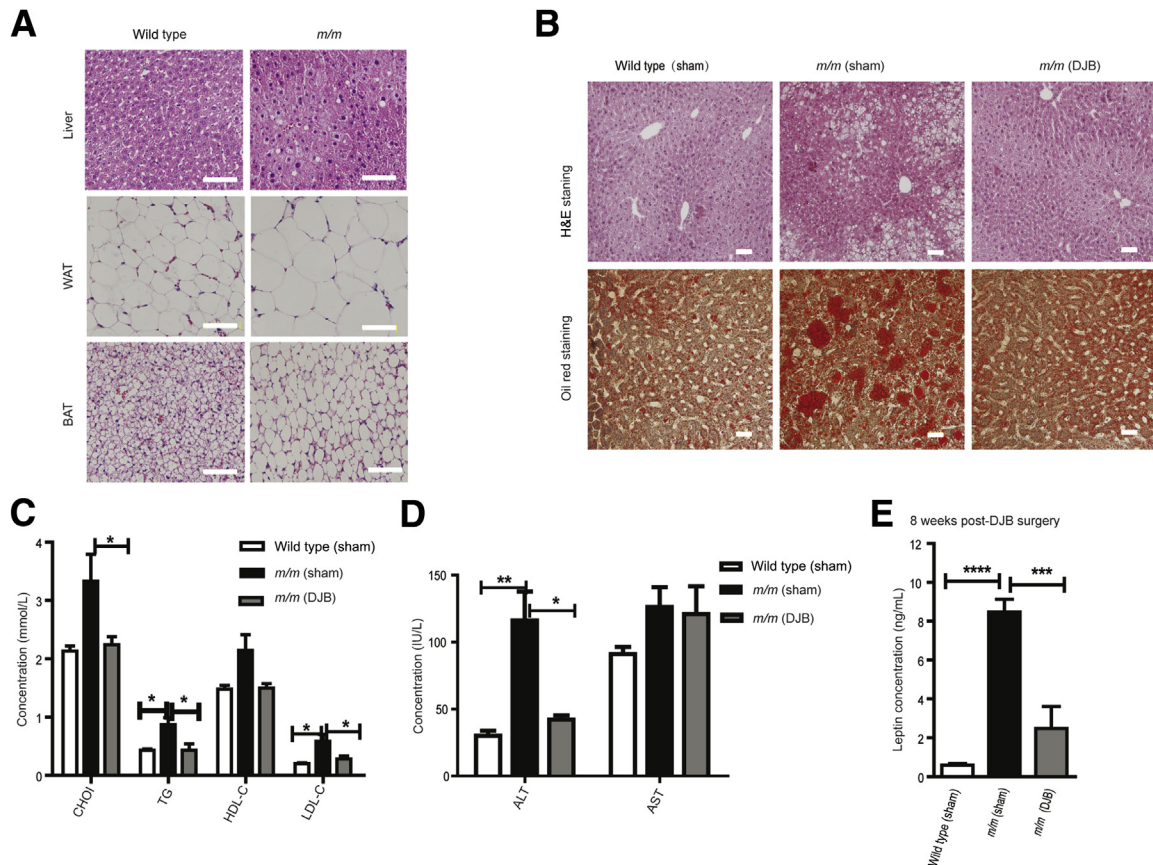


Figure 3 Lipid accumulation is reversed in livers of DJB male *Timo* mice. **A:** Representative H&E staining of liver, WAT, and BAT in 8-week-old male *Timo* mice. **B:** Representative H&E and oil red O staining of livers of *Timo* mice 9 weeks after DJB surgery. **C:** Plasma concentrations of CHOI, TG, HDL-C, and LDL-C of male *Timo* mice 9 weeks after DJB surgery. **D:** Representative enzymes of hepatitis (ALT, AST), which was partially reduced after surgery. **E:** Plasma leptin concentrations in the sham group and DJB mice by enzyme-linked immunosorbent assay. Data are expressed as means \pm SEM. $n = 3$ (**A**); $n = 3$ to 7 (**E**). * $P < 0.05$, ** $P < 0.005$, *** $P < 0.001$, and **** $P < 0.0005$. Scale bars: 50 μ m (**A**); 20 μ m (**B**). Original magnification, $\times 40$. ALT, alanine aminotransferase; AST, aspartate aminotransferase; BAT, brown adipocyte tissue; CHOI, cholesterol; DJB, duodenum-jejunum gastric bypass; HDL-C, high-density lipoprotein cholesterol; H&E, hematoxylin and eosin; LDL-C, low-density lipoprotein cholesterol; TG, triglycerides; WAT, white adipose tissue.

alleviated 9 weeks after DJB surgery, which contributed to the improvement in lipid metabolism (Figure 3D). We measured serum concentrations of total cholesterol, triglycerides, high-density lipoprotein, and very-low-density lipoprotein to investigate whether the decreased weight of *Timo* mice 9 weeks after DJB surgery reflected changes in lipid lysis. Total cholesterol and very-low-density lipoprotein decreased postoperatively in male and female *Timo* mice after DJB surgery (Figure 3C and Supplemental Figure S5B). Leptin concentrations in serum also decreased to normal concentrations in *Timo* mice 8 weeks after DJB surgery (Figure 3E).

Microbiota Alterations and Inflammation Suppression Results from DJB Surgery

Accumulating evidence indicates that bariatric surgery affects the diversity of gut microbiota.^{13,14,17} We analyzed fecal bacterial composition 1 week and 2 weeks after DJB surgery using denaturing gradient gel electrophoresis

analysis to examine immediate changes in gut microbiota. Fecal bacteria exhibited different dominant populations with lower diversity in DJB mice than in wild-type littermates. Bacterial communities were unstable, which was indicated by large variations in different samples (Figure 4A). Desulfovibrionaceae abundance was much higher in the sham group of *Timo* mice (Table 1 and Supplemental Figure S6A) 1 week after surgery, Clostridiales abundance decreased (Table 2, Supplemental Figure S6A), and Verrucomicrobiaceae abundance increased (Supplemental Figure S6A and Table 2) in *Timo* DJB mice 2 weeks after surgery. The predominant gut bacteria community became consistent within the same experimental group 2 weeks after DJB surgery. The increase in Verrucomicrobiaceae abundance was more significant in *Timo* DJB mice (Table 2, Supplemental Figure S6B).

We also sequenced the gut bacterial 16S rRNA gene variation region from the intestines of DJB *Timo* mice, sham *Timo* mice, and sham wild-type littermates 9 weeks after DJB surgery (Figure 4 and Supplemental Figure S7). A total

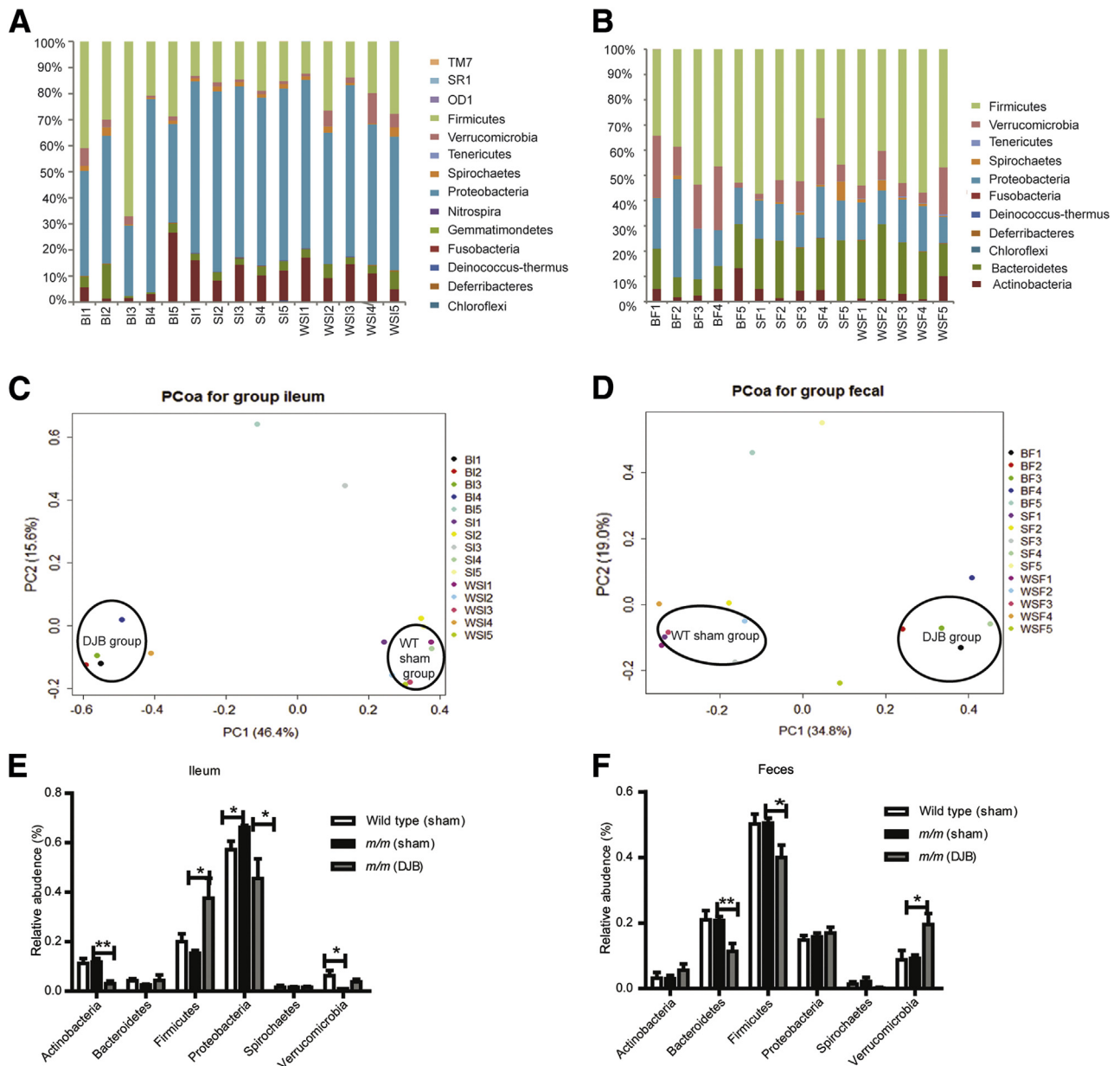


Figure 4 Average relative abundance of ileum and fecal bacterial orders in DJB and sham *Timo* mice. **A** and **B**: Ileum and fecal microbial composition of individual mice from sham control (SI/SF, WSI/WSF) and DJB-operated groups (BI/BF) 9 weeks after DJB surgery by microbiota 16S rRNA gene sequencing and analysis. **C** and **D**: Principal coordinates analysis plot of weighted UniFrac distances. Each dot represents ileum or fecal community in the sham group and DJB group, indicated by color. **E** and **F**: Relative abundance of different microbiota in ileum and fecal sample in DJB group and sham group. Data are expressed as means \pm SEM. $n = 5$. $*P < 0.05$, $**P < 0.005$. BI/BF, DJB-operated group; DJB, duodenum-jejunum gastric bypass; SI/SF, *Timo* sham group; WSI/WSF, wild-type sham group; WT, wild-type.

of 105 samples from 15 mice were analyzed (average 92,376 16S rRNA gene sequences per sample) (Supplemental Table S1). Principal coordinate analysis plots of weighted UniFrac distances demonstrated that DJB surgery exhibited stronger effects on gut microbiota in DJB *Timo* mice than in the sham mice (Figure 4, C and D), especially in distal small intestine (Figure 3, A and E, and Supplemental Figure S7, A and B), large intestine, and feces (Figure 4, B and F, and Supplemental Figure S7, C–E). We found a higher abundance of anti-inflammatory Firmicutes

and lower proinflammatory Proteobacteria in ileum in *Timo* mice 9 weeks after surgery (Figure 4E), but Verrucomicrobiaceae abundance increased significantly in the ileum and feces of *Timo* DJB mice (Figure 4, E and F). A decrease in the abundance of *Bacteroides* was observed in different parts of the large intestine (Figure 4F and Supplemental Figure S7, C–E). These data support that pathogenic bacteria decreased and beneficial microflora increased in *Timo* DJB mice, which may be associated with the improvements in the metabolism of *Timo* mice after DJB surgery.

Table 1 DGGE Band Analysis for 1 Week from the Feces of *Timo* Mice and Sham Control Mice after Surgery

No.	Domain	Phylum	Class	Order	Family	Genus	Identity (%)
1-1	Bacteria	Firmicutes	Clostridia	Clostridiales	Eubacteriaceae	<i>Eubacterium</i>	90
1-2	Bacteria	Verrucomicrobia	Verrucomicrobiae	Verrucomicrobiales	Verrucomicrobiaceae	<i>Akkermansia</i>	100
1-3	Bacteria	Firmicutes	Clostridia	Clostridiales	Lachnospiraceae		90
1-4	Bacteria	Firmicutes	Clostridia	Clostridiales	Lachnospiraceae	<i>Roseburia</i>	92
1-5	Bacteria	Firmicutes	Clostridia	Clostridiales	Lachnospiraceae		88
1-6	Bacteria	Firmicutes	Clostridia	Clostridiales	Lachnospiraceae	<i>Roseburia</i>	89
1-7	Bacteria	Proteobacteria	Deltaproteobacteria	Desulfovibrionales	Desulfovibrionaceae	<i>Lawsonia</i>	89
1-8	Bacteria	Firmicutes	Clostridia	Clostridiales	Lachnospiraceae	<i>Blautia</i>	91
1-9	Bacteria	Firmicutes	Clostridia	Clostridiales	Lachnospiraceae	<i>Roseburia</i>	88
1-10	Bacteria	Firmicutes	Clostridia	Clostridiales	Lachnospiraceae	<i>Roseburia</i>	95
1-11	Bacteria	Firmicutes	Clostridia	Clostridiales	Lachnospiraceae	<i>Roseburia</i>	94
1-12	Bacteria	Proteobacteria	Gammaproteobacteria	Enterobacteriales	Enterobacteriaceae	<i>Citrobacter</i>	94
1-13	Bacteria	Verrucomicrobia	Verrucomicrobiae	Verrucomicrobiales	Verrucomicrobiaceae	<i>Akkermansia</i>	100
1-14	Bacteria	Verrucomicrobia	Verrucomicrobiae	Verrucomicrobiales	Verrucomicrobiaceae	<i>Akkermansia</i>	100
1-15	Bacteria	Verrucomicrobia	Verrucomicrobiae	Verrucomicrobiales	Verrucomicrobiaceae	<i>Akkermansia</i>	99

DGGE, denaturing gradient gel electrophoresis.

DJB Surgery Suppressed Systemic Inflammation in *Timo* Mice

Systemic inflammation was reported in obese humans and many rodent models.^{11,15,20,30–32} Inflammation was observed in WAT, liver, BAT, and muscle tissue of adult *Timo* mice, as indicated by the up-regulation of macrophage markers and inflammatory cytokines (Figure 5, A and B, and Supplemental Figure S5, D and E). The up-regulation of active macrophage markers and proinflammatory cytokines in WAT, BAT, and skeletal muscle occurred at 4 weeks of age, which occurred before the significant increase in body weight at 6 weeks in male *Timo* mice (Figure 5A and Supplemental Figure S5, D and E), and liver inflammation occurred at a later stage (8 weeks) (Figure 5B). The

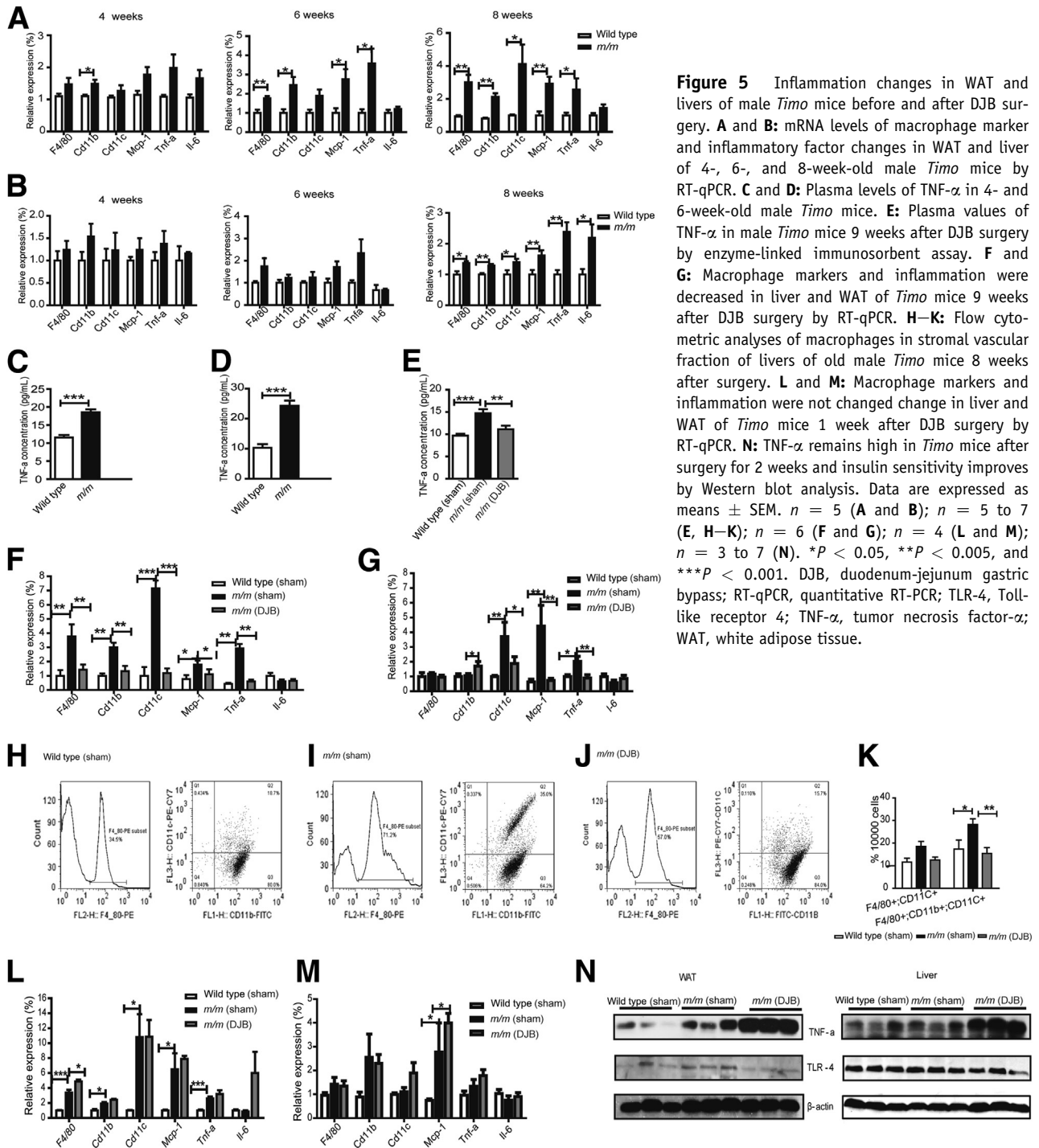
inflammation was aggravated with progression of obesity and diabetes in *Timo* mice, as indicated by the significant increase in the adipokines *Tnf- α* and *Mcp-1* at 8 weeks of age (Figure 5, A and B).

DJB surgery significantly ameliorated inflammation in the liver and WAT of *Timo* mice. The expression of macrophage markers (*F4/80*, *Cd11b*, and *Cd11c*) and proinflammatory cytokines (*Tnf- α* and *Mcp-1*) were significantly down-regulated 8 weeks after DJB surgery in the WAT and liver of *Timo* mice (Figure 5, F and G). Serum levels of *TNF- α* were also significantly lower than before DJB surgery (Figure 5, C–E). The number of macrophages in livers of *Timo* mice also decreased (Figure 5, H–K). To investigate whether inflammation alleviation resulted in insulin sensitivity improved in *Timo*

Table 2 DGGE Band Analysis from the Feces of *Timo* Mice and Sham Control Mice after Surgery for 2 Weeks

No.	Domain	Phylum	Class	Order	Family	Genus	Identity (%)
2-1	Bacteria	Firmicutes	Clostridia	Clostridiales	Lachnospiraceae	<i>Roseburia</i>	93
2-2	Bacteria	Firmicutes	Clostridia	Clostridiales	Eubacteriaceae	<i>Eubacterium</i>	89
2-3	Bacteria	Proteobacteria	Deltaproteobacteria	Desulfovibrionales	Desulfovibrionaceae	<i>Lawsonia</i>	89
2-4	Bacteria	Proteobacteria	Deltaproteobacteria	Desulfovibrionales	Desulfovibrionaceae	<i>Lawsonia</i>	89
2-5	Bacteria	Firmicutes	Clostridia	Clostridiales	Lachnospiraceae	<i>Roseburia</i>	91
2-6	Bacteria	Proteobacteria	Gammaproteobacteria	Enterobacteriales	Enterobacteriaceae	<i>Escherichia</i>	99
2-7	Bacteria	Firmicutes	Clostridia	Clostridiales	Ruminococcaceae	<i>Ruminococcus</i>	89
2-8	Bacteria	Firmicutes	Clostridia	Clostridiales	Lachnospiraceae	<i>Roseburia</i>	92
2-9	Bacteria	Firmicutes	Clostridia	Clostridiales	Lachnospiraceae	<i>Roseburia</i>	89
2-10	Bacteria	Proteobacteria	Deltaproteobacteria	Desulfovibrionales	Desulfovibrionaceae	<i>Desulfovibrio</i>	92
2-11	Bacteria	Firmicutes	Clostridia	Clostridiales	Eubacteriaceae	<i>Eubacterium</i>	88
2-12	Bacteria	Verrucomicrobia	Verrucomicrobiae	Verrucomicrobiales	Verrucomicrobiaceae	<i>Akkermansia</i>	100
2-13	Bacteria	Firmicutes	Clostridia	Clostridiales	Oscillospiraceae	<i>Oscillibacter</i>	91
2-14	Bacteria	Proteobacteria	Deltaproteobacteria	Desulfovibrionales	Desulfovibrionaceae	<i>Desulfovibrio</i>	92
2-15	Bacteria	Verrucomicrobia	Verrucomicrobiae	Verrucomicrobiales	Verrucomicrobiaceae	<i>Akkermansia</i>	99
2-16	Bacteria	Firmicutes	Clostridia	Clostridiales	Ruminococcaceae	<i>Ruminococcus</i>	90
2-17	Bacteria	Verrucomicrobia	Verrucomicrobiae	Verrucomicrobiales	Verrucomicrobiaceae	<i>Akkermansia</i>	99
2-18	Bacteria	Firmicutes	Clostridia	Clostridiales	Lachnospiraceae		92

DGGE, denaturing gradient gel electrophoresis.



mice, we studied the inflammation of WAT and liver of *Timo* mice 1 week after surgery. We found that the expression of macrophage markers (F4/80, Cd11b, and Cd11c) and proinflammatory cytokines (Tnf- α and Mcp-1) were not down-regulated, suggesting inflammation had not been suppressed (Figure 5, L and M). Furthermore, TNF- α expression was still elevated after DJB operation for 2 weeks (Figure 5N). This result supported the fact that the prominent long-time not short-time effects of DJB surgery

on glycemic control result in the alleviation of inflammation postoperatively.

DJB Surgery Did Not Affect *Bdnf* Transcript Level in Hypothalamus and Hippocampus

The lower expression of BDNF in *Timo* mice contributes to obesity and diabetes phenotypes.²¹ We measured mRNA levels and protein levels of *Bdnf* genes in the hypothalamus

and hippocampus of *Timo* mice after DJB surgery to investigate whether the reverse effects of DJB surgery were due to alterations in BDNF expression. No significant changes in *Bdnf* were observed in brains of *Timo* mice 9 weeks after DJB surgery (Figure 6, A and B), and BDNF protein levels increased in hypothalamus and hippocampus of *Timo* mice after DJB surgery but not in the peripheral system (Figure 6, C–E). Otherwise, no significant difference was observed in HFD-fed mice 9 weeks after surgery compared with sham control mice (Supplemental Figure S8).

To investigate whether the BDNF level change in *Timo* mice contributed to microbiota change, we examined the BDNF level in *Timo* mice after surgery for 1 week while its microbiota altered. Our results show that no significant change of BDNF occurred in *Timo* mice after DJB surgery for 1 week (Figure 6F). These data suggest that the BDNF change in DJB *Timo* mice was indirectly affected by insulin sensitivity improvement.

Discussion

More than a dozen major studies demonstrated that bariatric Roux-en-Y gastric bypass surgery is therapeutic in T2DM

human patients, rat, and mice by improving insulin sensitivity.^{6,17,33–35} Most research on gastric bypass was performed on HFD-fed rodent models.^{14,17,35,36} To our knowledge, the present work confirmed for the first time that DJB surgery effectively combats systemic inflammation and metabolic abnormalities in *Timo* mice, which is a *Bdnf* deficiency-induced T2DM model. In addition, we found the DJB surgery did not alter the expression of *Bdnf*, indicating a compensatory pathway for the DJB effects.

Accumulating evidence indicates that insulin resistance and lipid metabolism disorder are the hallmarks of obesity and contribute to the development of T2DM, cardiovascular disorders, and nonalcoholic fatty liver disease.^{2,9,37} Inflammation, especially in WAT and liver, is a key feature of obesity and T2DM.^{11,20} Individuals with increased levels of TNF- α and IL-6 exhibit insulin resistance.^{9,38} We also observed that systemic inflammation appeared before weight gain and insulin resistance in *Timo* mice. We found that DJB surgery significantly suppressed inflammation and TNF- α levels in *Timo* mice. This result is consistent with reports that barbaric surgery alleviated inflammation in mice with high sucrose–induced nonalcoholic steatohepatitis.³² However, inflammation alleviation was not the direct cause for improvements in the insulin sensitivity that

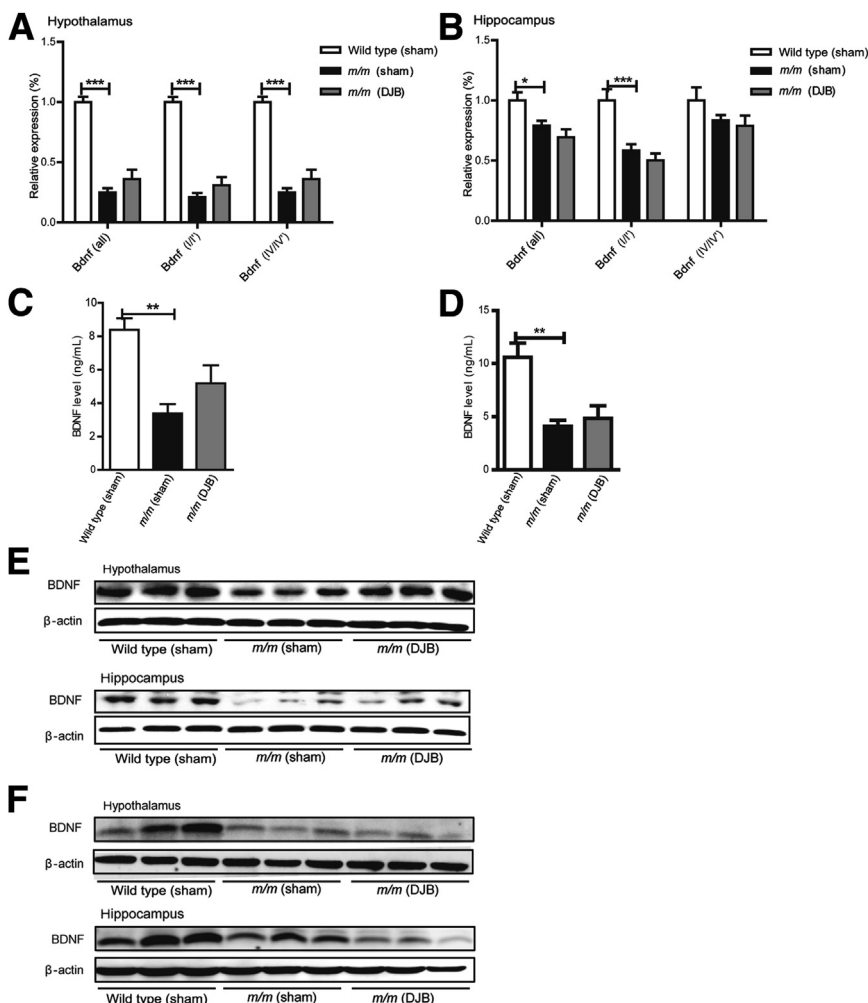


Figure 6 *Bdnf* level in different tissues of male *Timo* mice 9 weeks after surgery. *Bdnf* transcripts were determined using quantitative real-time RT-PCR. *Bdnf* transcripts I/I' and IV/IV' were investigated. **A** and **B**: Levels of different *Bdnf* transcripts in hypothalamus and hippocampus of DJB *Timo* mice and sham control mice by quantitative RT-PCR. All data are from 9 weeks after surgery in *Timo* mice. **C** and **D**: Plasma levels of BDNF in male *Timo* mice 2 and 9 weeks after DJB surgery by enzyme-linked immunosorbent assay. **E**: Protein levels of BDNF increase in hypothalamus and hippocampus of *Timo* mice 9 weeks after surgery by Western blot analysis. **F**: Protein levels of BDNF increase in hypothalamus and hippocampus of *Timo* mice 1 week after surgery by Western blot analysis. Data are expressed as means \pm SEM. $n = 6$ per group (**A** and **B**) * $P < 0.05$, ** $P < 0.05$, and *** $P < 0.001$. BDNF, brain-derived neurotrophic factor; DJB, duodenum-jejunum gastric bypass.

resulted from DJB surgery because enhanced insulin sensitivity preceded the TNF- α down-regulation. Inflammation reduction has been related to long-time intermittent deprivation of food both in mice and rat.^{39,40} However, all *Timo* mice after DJB surgery were only deprived of food one time (16 hours or 6 hours) for glucose tolerance test or insulin tolerance test and re-fed at least 2 weeks before inflammation measurement, we believed that food deprivation and re-feeding did not affect the conclusion about DJB effects on inflammation after DJB surgery. The lower inflammatory status may be beneficial for the maintenance of normal metabolic homeostasis because TNF- α administration partially impaired insulin sensitivity after DJB surgery in *Timo* mice (Supplemental Figure S5C).

An increasing abundance of Proteobacteria was involved in inflammation-associated dysbiosis.^{15,41} Studies suggested that the decreased abundance of *Bacteroides* and increase in Verrucomicrobia correlated with the enhancement of insulin sensitivity after bariatric surgery.^{3,13,14,17} Our data also demonstrated an increase in Proteobacteria in the ileum and feces of *Timo* mice (Figure 3, A, B and G), which is consistent with the up-regulated inflammation in *Timo* mice (Figure 4D). We observed an increase in the abundance of Verrucomicrobia (genus: *Akkermansia*) and decrease in Bacteroidetes in *Timo* mice after DJB surgery, and a significant change in Verrucomicrobia appeared before the insulin sensitivity improvement after DJB surgery for 1 week (Figure 3A and Figure 1K). TNF- α levels remained high in WAT and liver of DJB *Timo* mice at this time (Figure 4L). The higher abundance of Firmicutes in ileum demonstrated lipid metabolism improvements after DJB surgery. The time course of different physiologic events after surgery may indicate that microbiota abundance alterations, but not inflammation, directly suppressed the effects on obesity and diabetes.

One of the possibilities for metabolic improvements may be the direct or indirect influence of DJB on brain BDNF expression. We examined BDNF expression after DJB surgery to exclude this possibility. We did not observe significant changes in the hypothalamus or hippocampus of DJB *Timo* mice before its metabolism homeostasis improved (Figure 6F). Bercik et al⁴² found that the intestinal microbiota affects BDNF and behavior in BALB/c mice. Another group confirms that the gut microbiota affects hypothalamic and brainstem body fat—regulating circuits in C57Bl/6J male mice involved in reduction of leptin sensitivity and the expression of the obesity-suppressing neuropeptides proglucagon and Bdnf.⁴³ Therefore, current data suggest that the changes in insulin sensitivity, inflammation, and gut microbiota are independent of BDNF changes (Figures 5 and 6).

Our results revealed the role of inflammation and microbiota in the effects of DJB surgery, and these data indicated that suppressed inflammation is the result, not the cause, of diabetes reversal in *Timo* mice after DJB

surgery. Gut microbiota alterations may be the key reason for diabetes remission after DJB surgery, but more mechanistic studies are needed to explain how different families of microbiota regulate nutrient metabolism in the host. Given the potential role of microbiota in mediating inflammation, gut microbiota transplantation may become an effective treatment of enteritis and related bowel diseases.

Acknowledgments

S.J., Q.W., Z.H., A.S., Y.P., S.H., S.G., W.Z., and S.Y. performed experiments; S.J., Z.L., and X.G. designed the experiments and wrote the manuscript.

Supplemental Data

Supplemental material for this article can be found at <http://dx.doi.org/10.1016/j.ajpath.2016.04.009>.

References

- Despres JP, Lemieux I: Abdominal obesity and metabolic syndrome. *Nature* 2006, 444:881–887
- Van Gaal LF, Mertens IL, De Block CE: Mechanisms linking obesity with cardiovascular disease. *Nature* 2006, 444:875–880
- Zhang H, DiBaise JK, Zuccolo A, Kudrna D, Braidotti M, Yu Y, Parameswaran P, Crowell MD, Wing R, Rittmann BE, Krajmalnik-Brown R: Human gut microbiota in obesity and after gastric bypass. *Proc Natl Acad Sci U S A* 2009, 106:2365–2370
- Karra E, Youssef A, Batterham RL: Mechanisms facilitating weight loss and resolution of type 2 diabetes following bariatric surgery. *Trends Endocrinol Metab* 2010, 21:337–344
- Dirksen C, Bojsen-Moller KN, Jorgensen NB, Jacobsen SH, Kristiansen VB, Naver LS, Hansen DL, Worm D, Holst JJ, Madsbad S: Exaggerated release and preserved insulinotropic action of glucagon-like peptide-1 underlie insulin hypersecretion in glucose-tolerant individuals after Roux-en-Y gastric bypass. *Diabetologia* 2013, 56:2679–2687
- Ochner CN, Gibson C, Shanik M, Goel V, Geliebter A: Changes in neurohormonal gut peptides following bariatric surgery. *Int J Obes* 2011, 35:153–166
- Ashrafian H, le Roux CW: Metabolic surgery and gut hormones - a review of bariatric entero-humoral modulation. *Physiol Behav* 2009, 97:620–631
- Suzuki K, Simpson KA, Minnion JS, Shillito JC, Bloom SR: The role of gut hormones and the hypothalamus in appetite. *Endocr J* 2010, 57:359–372
- Olefsky JM, Glass CK: Macrophages, inflammation, and insulin resistance. *Annu Rev Physiol* 2010, 72:219–246
- Gregor MF, Hotamisligil GS: Inflammatory mechanisms in obesity. *Annu Rev Immunol* 2011, 29:415–445
- Talukdar S, Oh da Y, Bandyopadhyay G, Li D, Xu J, McNelis J, Lu M, Li P, Yan Q, Zhu Y, Ofrecio J, Lin M, Brenner MB, Olefsky JM: Neutrophils mediate insulin resistance in mice fed a high-fat diet through secreted elastase. *Nat Med* 2012, 18:1407–1412
- Henao-Mejia J, Elinav E, Jin C, Hao L, Mehal WZ, Strowig T, Thaïss CA, Kau AL, Eisenbarth SC, Jurczak MJ, Camporez JP, Shulman GI, Gordon JI, Hoffman HM, Flavell RA: Inflammasome-mediated dysbiosis regulates progression of NAFLD and obesity. *Nature* 2012, 482:179–185

13. Ryan KK, Tremaroli V, Clemmensen C, Kovatcheva-Datchary P, Myronovych A, Karns R, Wilson-Perez HE, Sandoval DA, Kohli R, Backhed F, Seeley RJ: FXR is a molecular target for the effects of vertical sleeve gastrectomy. *Nature* 2014, 509:183–188
14. Liou AP, Paziuk M, Luevano JM Jr, Machineni S, Turnbaugh PJ, Kaplan LM: Conserved shifts in the gut microbiota due to gastric bypass reduce host weight and adiposity. *Sci Transl Med* 2013, 5:178ra41
15. Le Chatelier E, Nielsen T, Qin J, Prifti E, Hildebrand F, Falony G, Almeida M, Arumugam M, Batto JM, Kennedy S, Leonard P, Li J, Burgdorf K, Grarup N, Jorgensen T, Brandslund I, Nielsen HB, Juncker AS, Bertalan M, Levenez F, Pons N, Rasmussen S, Sunagawa S, Tap J, Tims S, Zoetendal EG, Brunak S, Clement K, Dore J, Kleerebezem M, Kristiansen K, Renault P, Sicheritz-Ponten T, de Vos WM, Zucker JD, Raes J, Hansen T; MetaHIT consortium, Bork P, Wang J, Ehrlich SD, Pedersen O: Richness of human gut microbiome correlates with metabolic markers. *Nature* 2013, 500:541–546
16. Furet JP, Kong LC, Tap J, Poitou C, Basdevant A, Bouillot JL, Mariat D, Corthier D, Doré J, Henegar C, Rizkalla S, Clément K: Differential adaptation of human gut microbiota to bariatric surgery-induced weight loss: links with metabolic and low-grade inflammation markers. *Diabetes* 2010, 59:3049–3057
17. Li JV, Ashrafian H, Buetter M, Kinross J, Sands C, le Roux CW, Bloom SR, Darzi A, Athanasiou T, Marchesi JR, Nicholson JK, Holmes E: Metabolic surgery profoundly influences gut microbial-host metabolic cross-talk. *Gut* 2011, 60:1214–1223
18. Nadal I, Santacruz A, Marcos A, Warnberg J, Garagorri JM, Moreno LA, Martín-Matillas M, Campoy C, Martí A, Moleres A, Delgado M, Veiga OL, García-Fuentes M, Redondo CG, Sanz Y: Shifts in clostridia, bacteroides and immunoglobulin-coating fecal bacteria associated with weight loss in obese adolescents. *Int J Obes (Lond)* 2009, 33:758–767
19. Ding S, Chi MM, Scull BP, Rigby R, Schwerbrock NM, Magness S, Jobin C, Lund PK: High-fat diet: bacteria interactions promote intestinal inflammation which precedes and correlates with obesity and insulin resistance in mouse. *PLoS One* 2010, 5:e12191
20. Lee YS, Li P, Huh JY, Hwang JJ, Lu M, Kim JJ, Ham M, Talukdar S, Chen A, Lu WJ, Bandyopadhyay GK, Schwendener R, Olefsky J, Kim JB: Inflammation is necessary for long-term but not short-term high-fat diet-induced insulin resistance. *Diabetes* 2011, 60:2474–2483
21. Sha H, Xu J, Tang J, Ding J, Gong J, Ge X, Kong D, Gao X: Disruption of a novel regulatory locus results in decreased Bdnf expression, obesity, and type 2 diabetes in mice. *Physiol Genomics* 2007, 31:252–263
22. Woods M, Lan Z, Li J, Wheeler MB, Wang H, Wang R: Anti-diabetic effects of duodenojejunal bypass in an experimental model of diabetes induced by a high-fat diet. *Br J Surg* 2011, 98:686–696
23. Arkan MC, Hevener AL, Greten FR, Maeda S, Li ZW, Long JM, Wynshaw-Boris A, Poli G, Olefsky J, Karin M: IKK-beta links inflammation to obesity-induced insulin resistance. *Nat Med* 2005, 11:191–198
24. Huber JA, Mark Welch DB, Morrison HG, Huse SM, Neal PR, Butterfield DA, Sogin ML: Microbial population structures in the deep marine biosphere. *Science* 2007, 318:97–100
25. Junemann S, Prior K, Szczepanowski R, Harks I, Ehmke B, Goesmann A, Stoye J, Harmsen D: Bacterial community shift in treated periodontitis patients revealed by ion torrent 16S rRNA gene amplicon sequencing. *PloS ONE* 2012, 7:e41606
26. Kashyap SR, Gattaman P, Brethauer S, Schauer P: Bariatric surgery for type 2 diabetes: weighing the impact for obese patients. *Cleve Clin J Med* 2010, 77:468–476
27. Rubino F, Schauer PR, Kaplan LM, Cummings DE: Metabolic surgery to treat type 2 diabetes: clinical outcomes and mechanisms of action. *Annu Rev Med* 2010, 61:393–411
28. Xu H, Barnes GT, Yang Q, Tan G, Yang D, Chou CJ, Sole J, Nichols A, Ross JS, Tartaglia LA, Chen H: Chronic inflammation in fat plays a crucial role in the development of obesity-related insulin resistance. *J Clin Invest* 2003, 112:1821–1830
29. Saltiel AR, Kahn CR: Insulin signalling and the regulation of glucose and lipid metabolism. *Nature* 2001, 414:799–806
30. Amar S, Zhou Q, Shaik-Dasthagirisahab Y, Leeman S: Diet-induced obesity in mice causes changes in immune responses and bone loss manifested by bacterial challenge. *Proc Natl Acad Sci U S A* 2007, 104:20466–20471
31. Targher G, Bertolini L, Rodella S, Tessari R, Zenari L, Lippi G, Arcaro G: Nonalcoholic fatty liver disease is independently associated with an increased incidence of cardiovascular events in type 2 diabetic patients. *Diabetes Care* 2007, 30:2119–2121
32. Verbeek J, Lannoo M, Pirinen E, Ryu D, Spincemaille P, Vander Elst I, Windmolders P, Thevissen K, Cammue BP, van Pelt J, Fransis S, Van Eyken P, Ceuterick-De Groote C, Van Veldhoven PP, Bedossa P, Nevens F, Auwerx J, Cassiman D: Roux-en-y gastric bypass attenuates hepatic mitochondrial dysfunction in mice with non-alcoholic steatohepatitis. *Gut* 2015, 64:673–683
33. Barres R, Kirchner H, Rasmussen M, Yan J, Kantor FR, Krook A, Naslund E, Zierath JR: Weight loss after gastric bypass surgery in human obesity remodels promoter methylation. *Cell Rep* 2013, 3:1020–1027
34. Grayson BE, Schneider KM, Woods SC, Seeley RJ: Improved rodent maternal metabolism but reduced intrauterine growth after vertical sleeve gastrectomy. *Sci Transl Med* 2013, 5:199ra112
35. Salinari S, le Roux CW, Bertuzzi A, Rubino F, Mingrone G: Duodenal-jejunal bypass and jejunectomy improve insulin sensitivity in Goto-Kakizaki diabetic rats without changes in incretins or insulin secretion. *Diabetes* 2014, 63:1069–1078
36. Rasmussen BA, Breen DM, Duca FA, Cote CD, Zadeh-Tahmasebi M, Filippi BM, Lam TK: Jejunal leptin-PI3K signaling lowers glucose production. *Cell Metab* 2014, 19:155–161
37. Hotamisligil GS: Inflammation and metabolic disorders. *Nature* 2006, 444:860–867
38. Shi H, Kokoeva MV, Inouye K, Tzameli I, Yin H, Flier JS: TLR4 links innate immunity and fatty acid-induced insulin resistance. *J Clin Invest* 2006, 116:3015–3025
39. Vasconcelos AR, Yshii LM, Viel TA, Buck HS, Mattson MP, Scavone C, Kawamoto EM: Intermittent fasting attenuates lipopolysaccharide-induced neuroinflammation and memory impairment. *J Neuroinflammation* 2014, 11:85
40. Lara-Padilla E, Godinez-Victoria M, Drago-Serrano ME, Reyna-Garfias H, Arciniega-Martinez IM, Abarca-Rojano E, Cruz-Hernandez TR, Campos-Rodriguez R: Intermittent fasting modulates IgA levels in the small intestine under intense stress: a mouse model. *J Neuroimmunol* 2015, 285:22–30
41. Carvalho FA, Koren O, Goodrich JK, Johansson ME, Nalbantoglu I, Aitken JD, Su Y, Chassaing B, Walters WA, Gonzalez A, Clemente JC, Cullender TC, Barnich N, Darfeuille-Michaud A, Vijay-Kumar M, Knight R, Ley RE, Givortz AT: Transient inability to manage proteobacteria promotes chronic gut inflammation in TLR5-deficient mice. *Cell Host Microbe* 2012, 12:139–152
42. Bercik P, Denou E, Collins J, Jackson W, Lu J, Jury J, Deng Y, Blennerhassett P, Macri J, McCoy KD, Verdu EF, Collins SM: The intestinal microbiota affect central levels of brain-derived neurotrophic factor and behavior in mice. *Gastroenterology* 2011, 141:599–609. 609.e1–e3
43. Schele E, Grahnmemo L, Anesten F, Hallen A, Backhed F, Jansson JO: The gut microbiota reduces leptin sensitivity and the expression of the obesity-suppressing neuropeptides proglucagon (Gcg) and brain-derived neurotrophic factor (Bdnf) in the central nervous system. *Endocrinology* 2013, 154:3643–3651